



# A hardware implementation of the Levinson routine in the radio detector of cosmic rays to improve a suppression of non-stationary RFI

Zbigniew Szadkowski<sup>1</sup> IEEE Member, for the Pierre Auger Collaboration  
<sup>1</sup> University of Łódź, Poland

## ABSTRACT

The radio detector system for ultra high-energy cosmic rays in the Pierre Auger Observatory operates in the frequency range 30-80 MHz, which is often contaminated by human-made RFI. Several filters were used to suppress the RFI: based on the FFT, IIR notch filter and FIR filter based on the linear prediction. The last refreshes the FIR coefficients calculating either in the external ARM processor, internal soft-core NIOS<sup>®</sup> processor implemented inside the FPGA or hard-core embedded processors (HPS) being a silicon part of the FPGA chip. Refreshment times significantly depend on the type of calculation process. For stationary RFI, the FIR coefficients can be refreshed each minute or rarer. However, an efficient suppression of non-stationary short-term contaminations requires a much faster response. Calculations of FIR coefficients in an external ARM take 1-2 seconds, by the soft-core virtual NIOS<sup>®</sup> processor on the level of hundreds milliseconds. The HPS allows a reduction of refreshment time to  $\sim 20$  ms (for 32-stage FIR filter). A symmetry of covariance matrix allows one to use the much faster Levinson procedure instead of typical Gauss routine for solving a set of linear equations. The Levinson procedure calculated even in the HPS takes relatively a lot of time. A hardware implementation of this procedure inside the FPGA fabric as specialized a micro-controller requires only  $\sim 53$  800 clock cycles. We used 64- or 48-bit floating-point representations to calculate FIR coefficients. Resources occupation is relatively high, as the design was optimized for a maximal register performance. However, the RFI suppression is very efficient. We expect significant suppression of even short-term non-stationary RFI.

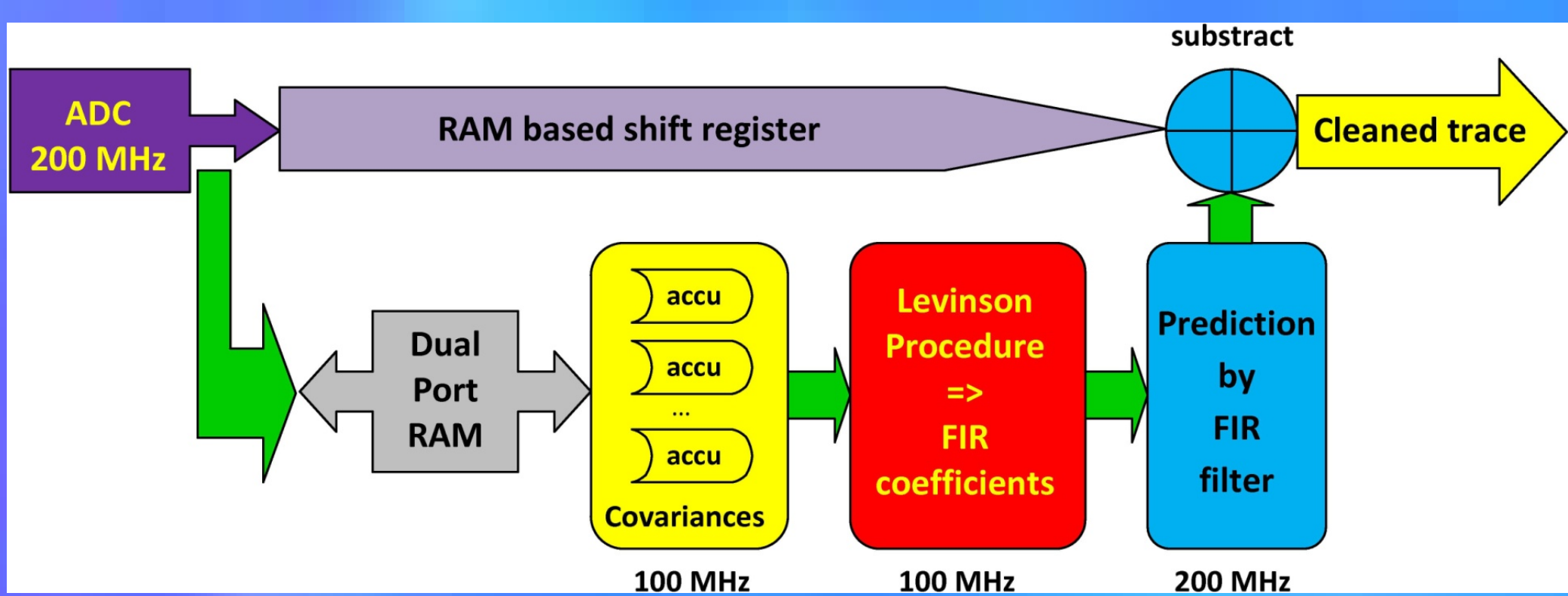


Fig. 1 – The structure of data flow for the hardware implementation of the Levinson algorithm.

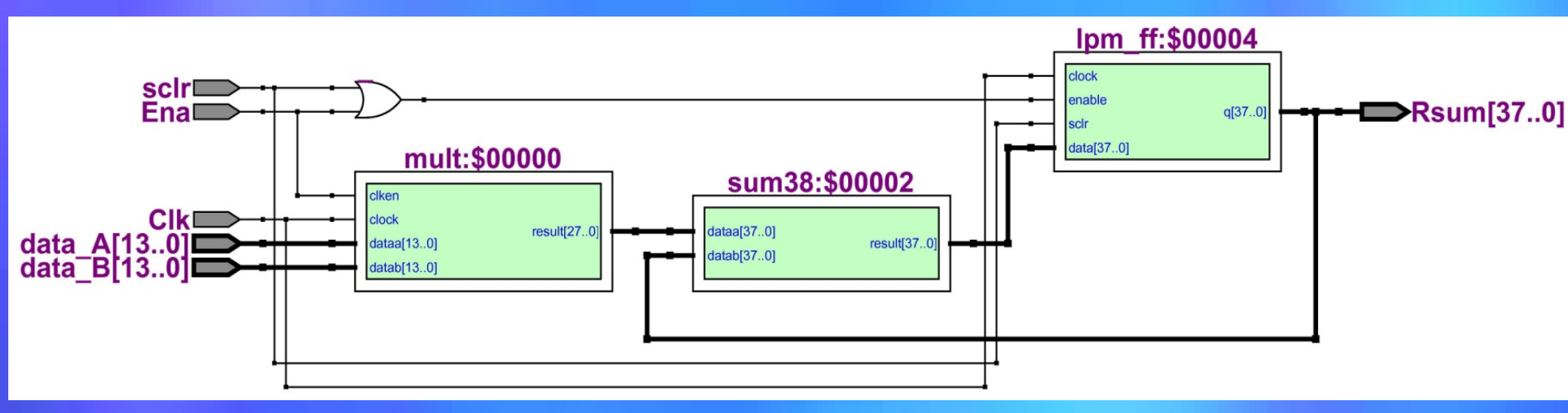


Fig. 2 – A structure of 32 fast logic blocks calculating covariances (as in Fig. 1). All data are the fixed-point representation.

	Loop A	Loop B	Loop C	Loop D
n=1	xi = 0; xi -= r[1] * a[0]; xi /= e;	a[1] = 0; a[1] += a[0] * xi;	z = y[1]; z -= r[1] * x[0]; pm = z/e;	x[1] = 0; x[0] += a[1] * pm; x[1] += a[0] * pm;
n=2	xi = 0; xi -= r[2] * a[0]; xi -= r[1] * a[1]; xi /= e;	a[2] = 0; a[2] += a[0] * xi; a[1] += a[1] * xi;	z = y[2]; z -= r[2] * x[0]; z -= r[1] * x[1]; pm = z/e;	x[2] = 0; x[0] += a[2] * pm; x[1] += a[1] * pm; x[2] += a[0] * pm;
n=3	xi = 0; xi -= r[3] * a[0]; xi -= r[2] * a[1]; xi -= r[1] * a[2]; xi /= e;	a[3] = 0; a[3] += a[0] * xi; a[2] += a[1] * xi; a[1] += a[2] * xi;	z = y[3]; z -= r[3] * x[0]; z -= r[2] * x[1]; z -= r[1] * x[2]; pm = z/e;	x[3] = 0; x[0] += a[3] * pm; x[1] += a[2] * pm; x[2] += a[1] * pm; x[3] += a[0] * pm;
n=4	xi = 0; xi -= r[4] * a[0]; xi -= r[3] * a[1]; xi -= r[2] * a[2]; xi -= r[1] * a[3]; xi /= e;	a[4] = 0; a[4] += a[0] * xi; a[3] += a[1] * xi; a[2] += a[2] * xi; a[1] += a[3] * xi;	z = y[4]; z -= r[4] * x[0]; z -= r[3] * x[1]; z -= r[2] * x[2]; z -= r[1] * x[3]; pm = z/e;	x[4] = 0; x[0] += a[4] * pm; x[1] += a[3] * pm; x[2] += a[2] * pm; x[3] += a[1] * pm; x[4] += a[0] * pm;
etc				

Fig. 4 – Four first steps in the Levinson algorithm implementation

```
void levinson(double *r, double *y, double *a, unsigned int dim)
{
    unsigned int n, i;
    double e, z, xi, temp;
    // initialization step //
    e = r[0];
    x[0] = y[0]/e;
    // main loop //
    for (n = 1; n < dim; ++n)
    // calculate xi //
    xi = 0;
    for (i = 0; i < n; ++i)
    { // loop A //
        xi += r[n-i] * a[i];
    }
    xi = xi/e;
    // update a //
    for (i = 0; i <= (n-1)/2; ++i)
    { // loop B //
        temp = a[i];
        a[i] = temp + a[n-i] * xi;
        a[n-i] = temp * xi;
    }
    if (n div 2 == 0)
    { // loop C //
        a[i] = a[i] + a[n-i] * xi;
    }
    // calculate e //
    e = e * (1 - xi*xi);
    // calculate l //
    for (i = 0; i < n; ++i)
    { // loop D //
        z = y[i];
        z -= r[n-i] * x[i];
    }
    // update x //
    x[n] = 0;
    for (i = 0; i <= n; ++i)
    { // loop D //
        x[i] += a[n-i] * z/e;
    }
    return;
}
```

Fig. 3 – C code of the Levinson algorithm.

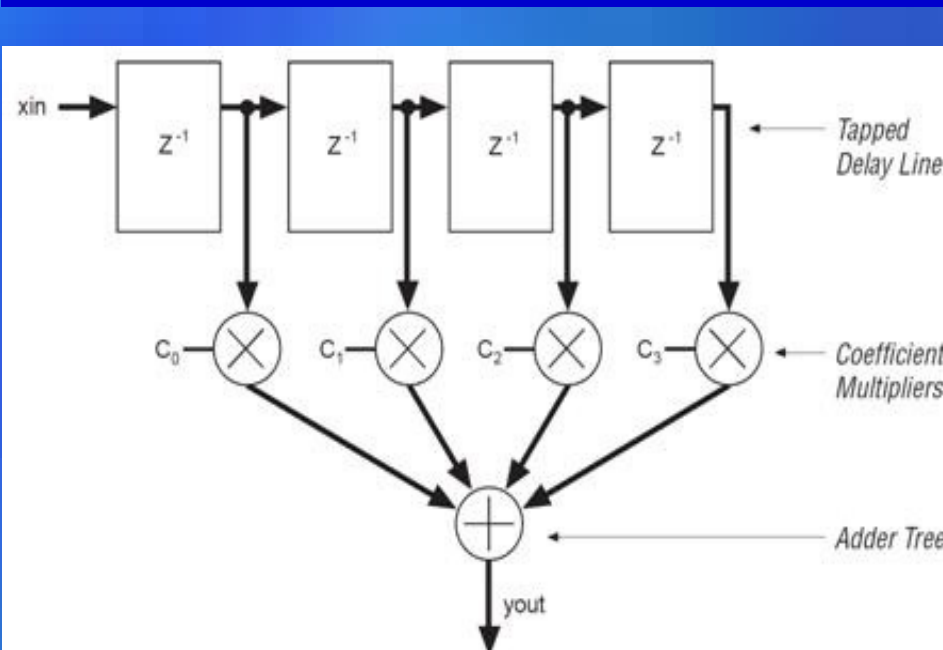


Fig. 5 – The structure of the FIR filter.

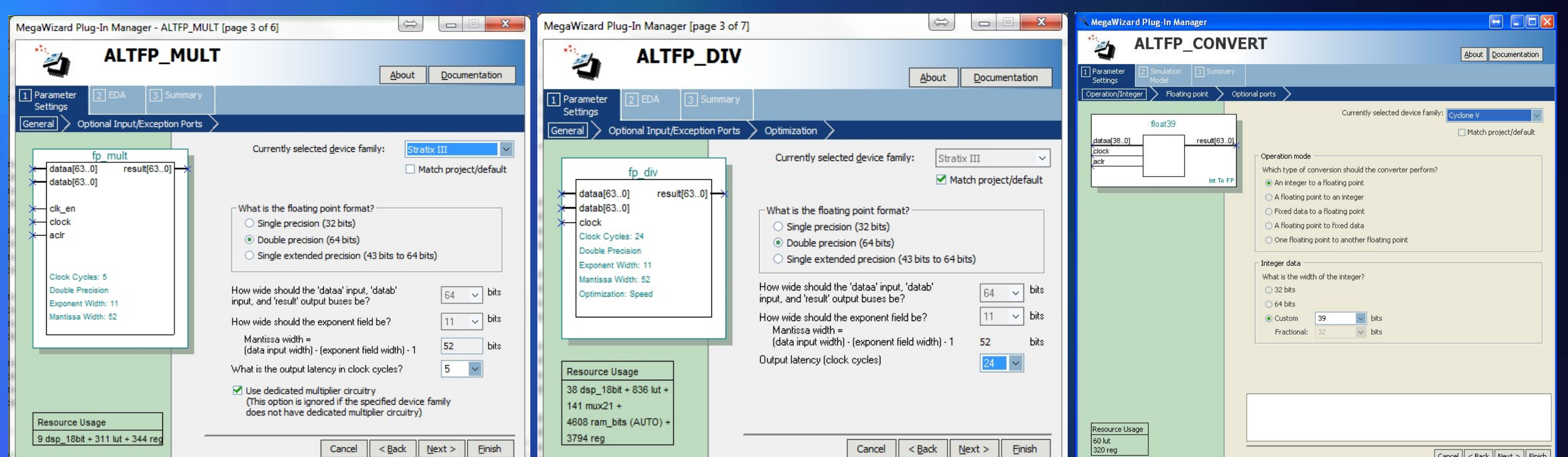


Fig. 8 – Altera® mega-functions multiplying, dividing and converting floating-point 64-bit variables.

A4...A0	Addr	Data	A4...A0	Addr	Data	A4...A0	Addr	Data	A4...A0	Addr	Data
00000	0	C18B90FA1000000	00000	0	C18B90FA100	00000	0	BF607586C27DED	00000	0	BF607586C27DED
00001	1	C18B90FA1000000	00001	1	C18B90FA100	00001	1	3FA579E6A740A43	00001	1	3FA579E6A740A43
00010	2	C18B90FA1000000	00010	2	C18B90FA100	00010	2	12F38D2E2E2E2E2E	00010	2	12F38D2E2E2E2E2E
00011	3	C18B90FA1000000	00011	3	C18B90FA100	00011	3	9D93A0C848139C	00011	3	9D93A0C848139C
00100	4	C18B90FA1000000	00100	4	C18B90FA100	00100	4	4656A3BE54885	00100	4	4656A3BE54885
00101	5	C18B90FA1000000	00101	5	C18B90FA100	00101	5	CD412E9BB7731	00101	5	CD412E9BB7731
00110	6	C18B90FA1000000	00110	6	C18B90FA100	00110	6	3D044E356480A	00110	6	3D044E356480A
00111	7	C18B90FA1000000	00111	7	C18B90FA100	00111	7	D7E5DC7A7C038	00111	7	D7E5DC7A7C038
01000	8	C18B90FA1000000	01000	8	C18B90FA100	01000	8	5A695C7E31657	01000	8	5A695C7E31657
01001	9	C18B90FA1000000	01001	9	C18B90FA100	01001	9	C0B680B87F5E1	01001	9	C0B680B87F5E1
01010	10	C18B90FA1000000	01010	10	C18B90FA100	01010	10	9D5F1546EF95B	01010	10	9D5F1546EF95B
01011	11	C18B90FA1000000	01011	11	C18B90FA100	01011	11	895F3ACB7C066	01011	11	895F3ACB7C066
01100	12	C18B90FA1000000	01100	12	C18B90FA100	01100	12	3806BF55DA0C7	01100	12	3806BF55DA0C7
01101	13	C18B90FA1000000	01101	13	C18B90FA100	01101	13	35D93444F2774	01101	13	35D93444F2774
01110	14	C18B90FA1000000	01110	14	C18B90FA100	01110	14	8A7F128440296	01110	14	8A7F128440296
01111	15	C18B90FA1000000	01111	15	C18B90FA100	01111	15	98BF4D95F382	01111	15	98BF4D95F382
10000	16	C18B90FA1000000	10000	16	C18B90FA100	10000	16	3FA579E6A740A43	10000	16	3FA579E6A740A43
10001	17	C18B90FA1000000	10001	17	C18B90FA100	10001	17	12F38D2E2E2E2E2E	10001	17	12F38D2E2E2E2E2E
10010	18	C18B90FA1000000	10010	18	C18B90FA100	10010	18	9D93A0C848139C	10010	18	9D93A0C848139C
10011	19	C18B90FA1000000	10011	19	C18B90FA100	10011	19	4656A3BE54885	10011	19	4656A3BE54885
10100	20	C18B90FA1000000	10100	20	C18B90FA100	10100	20	CD412E9BB7731	10100	20	CD412E9BB7731
10101	21	C18B90FA1000000	10101	21	C18B90FA100	10101	21	3D044E356480A	10101	21	3D044E356480A
10110	22	C18B90FA1000000	10110	22	C18B90FA100	10110	22	D7E5DC7A7C038	10110	22	D7E5DC7A7C038
10111	23	C18B90FA1000000	10111	23	C18B90FA100	10111	23	5A695C7E31657	10111	23	5A695C7E31657
11000	24	C18B90FA1000000	11000	24	C18B90FA100	11000	24	C0B680B87F5E1	11000	24	C0B680B87F5E1
11001	25	C18B90FA1000000	11001	25	C18B90FA100	11001	25	9D5F1546EF95B	11001	25	9D5F1546EF95B
11010	26	C18B90FA1000000	11010	26	C18B90FA100	11010	26	895F3ACB7C066	11010	26	895F3ACB7C066
11011	27	C18B90FA1000000	11011	27	C18B90FA100	11011	27	3806BF55DA0C7	11011	27	3806BF55DA0C7
11100	28	C18B90FA1000000	11100	28	C18B90FA100	11100	28	35D93444F2774	11100	28	35D93444F2774
11101	29	C18B90FA1000000	11101	29	C18B90FA100	11101	29	8A7F128440296	11101	29	8A7F128440296
11110	30	C18B90FA1000000	11110	30	C18B90FA100	11110	30	98BF4D95F382	11110	30	98BF4D95F382
11111	31	C18B90FA1000000	11111	31	C18B90FA100	11111	31	3FA579E6A740A43	11111	31	3FA579E6A740A43

Fig. 9 – Comparison of 64- and 48-bit input covariances (two left columns), FIR coefficients calculated in the PC (middle column) and in the FPGA 64-bit (4th column) and 48-bit (right column). Some discrepancy on least significant bits for 64-bit calculations are visible. However, the relative accuracy is on a level of 10<sup>-13</sup>. The accuracy for 48-bit calculations dramatically drops down to a level of 10<sup>-2</sup>.

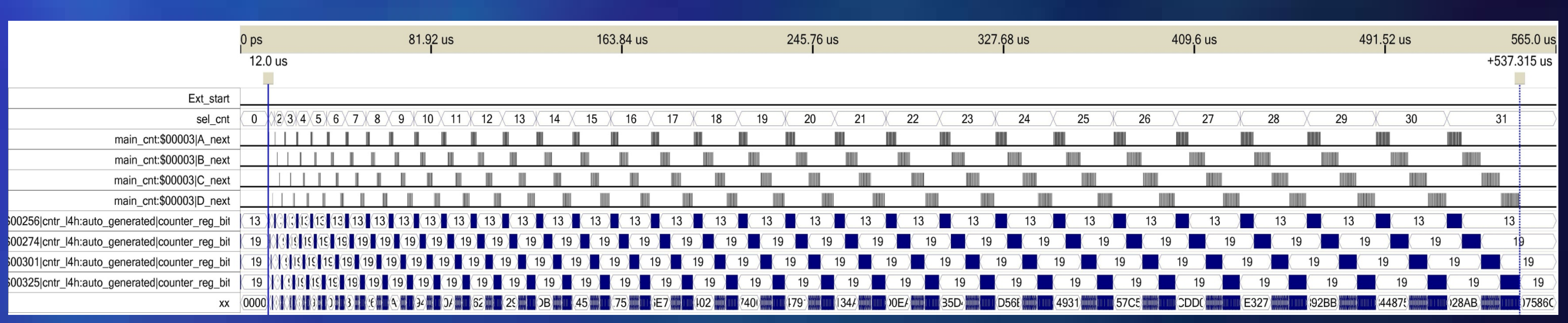


Fig. 10 – Quartus® simulation of FIR coefficients calculation by the hardware Levinson procedure. Calculation of  $r$  and  $y$  covariances takes 12  $\mu$ s, calculation of 64-bit floating-point coefficients takes next  $\sim 238$   $\mu$ s. Simulations show sequences of processing in the consecutive A, B, C and D loops.

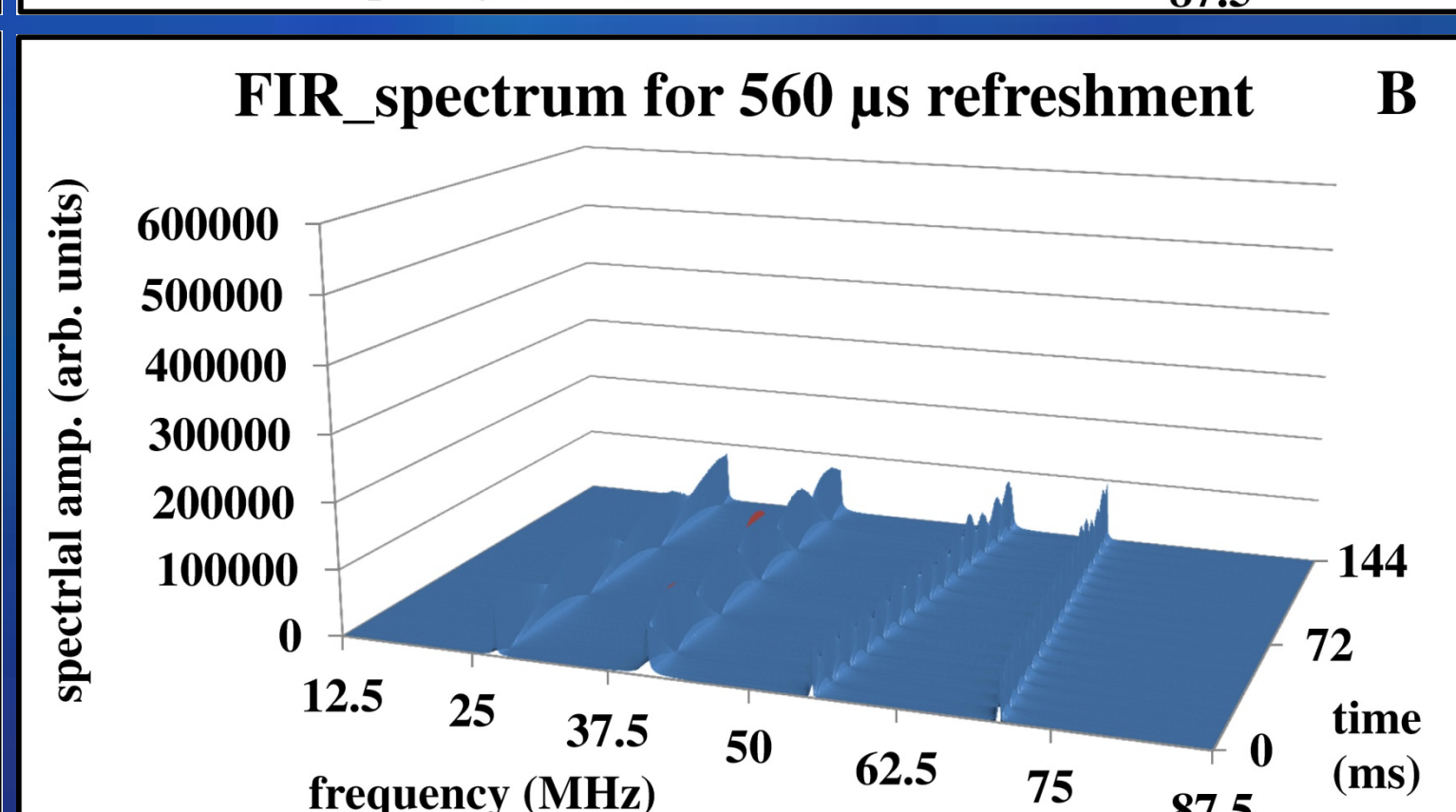
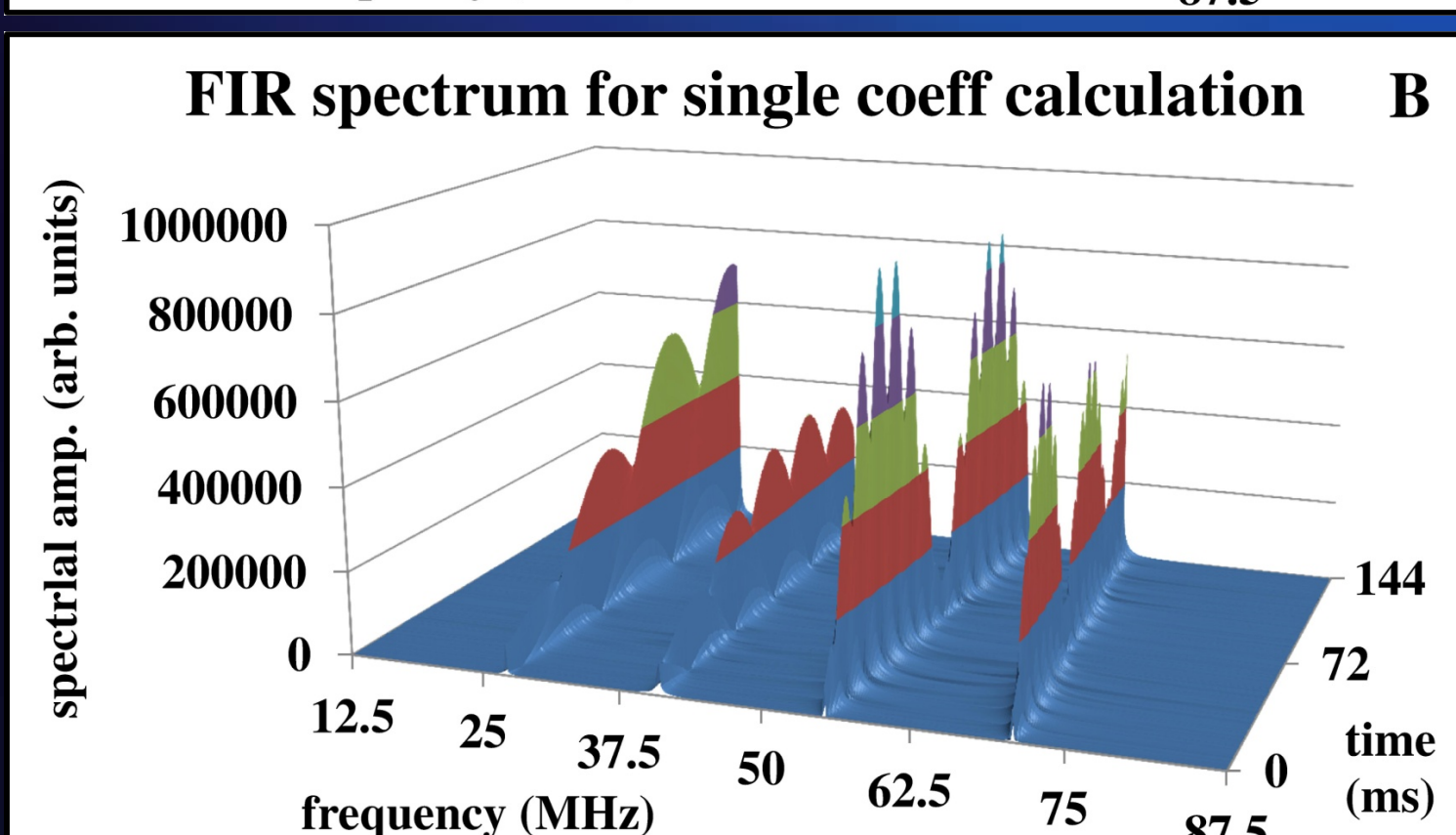
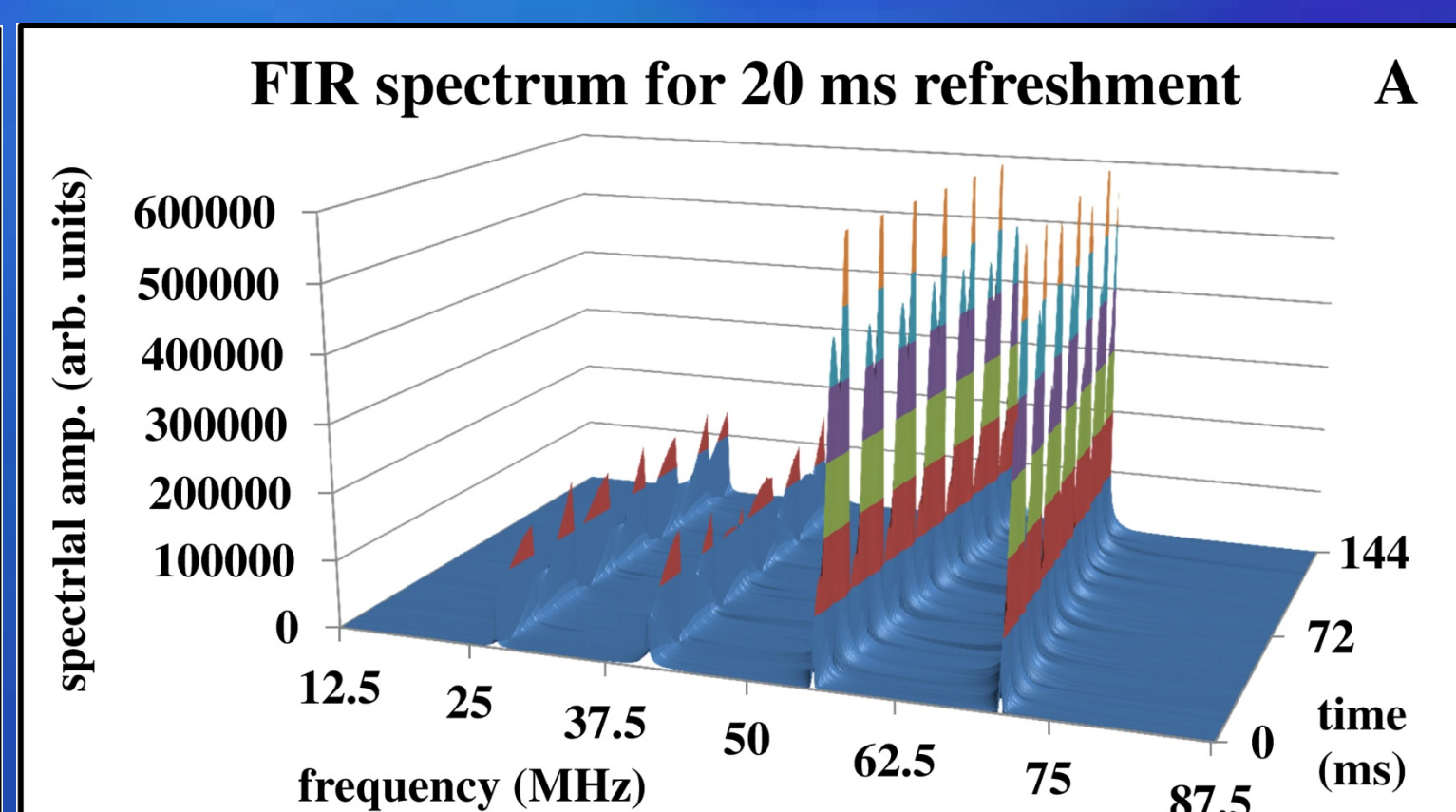
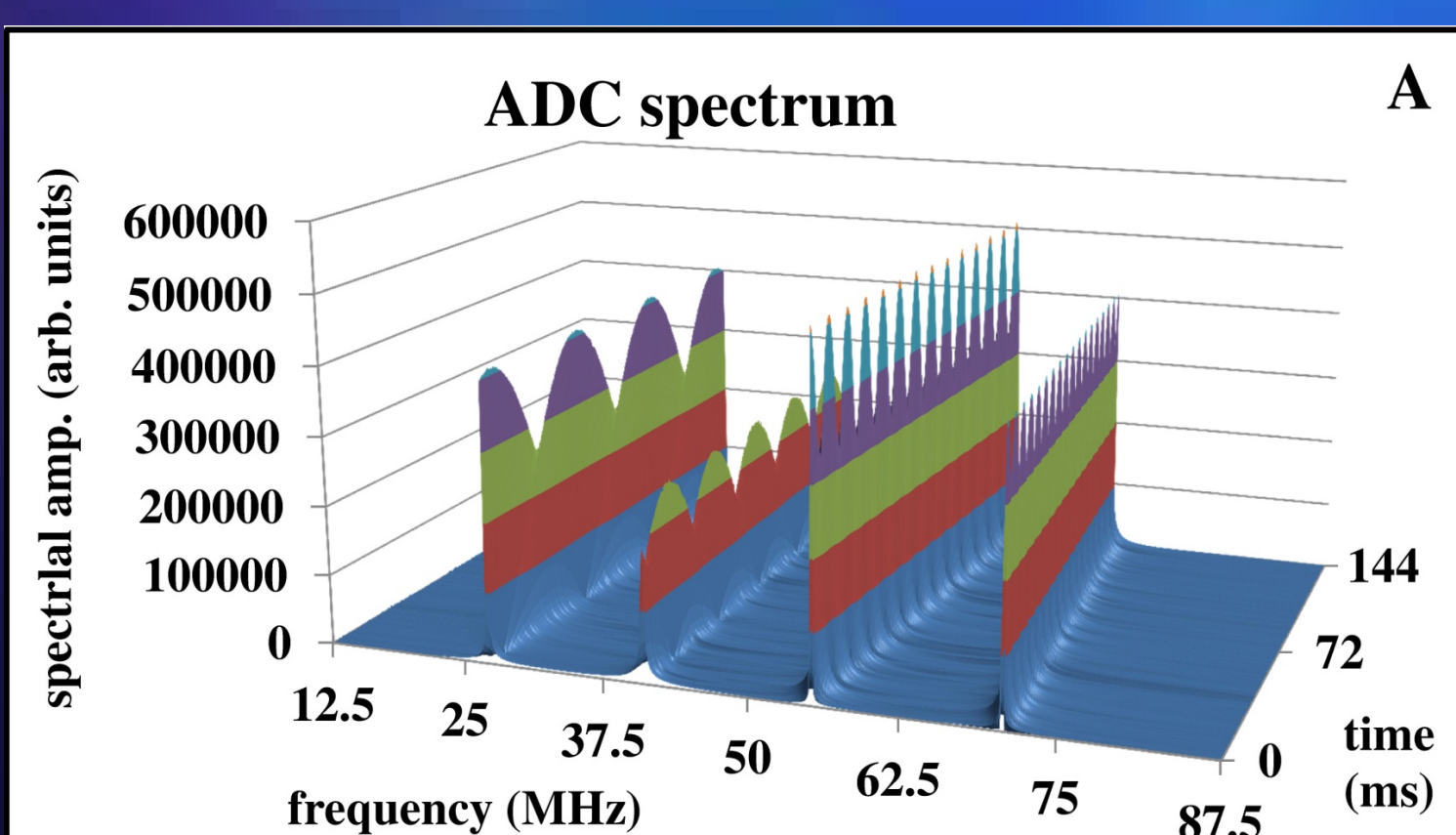


Fig. 6 – Fourier spectra for the original signal (A) and for a single calculation of FIR coefficients (B) in the beginning of trace cleaning.

Fig. 7 – Modules of Fourier spectra for a refreshment of FIR coefficients each 20 ms (A) and for each 560  $\mu$ s (B).

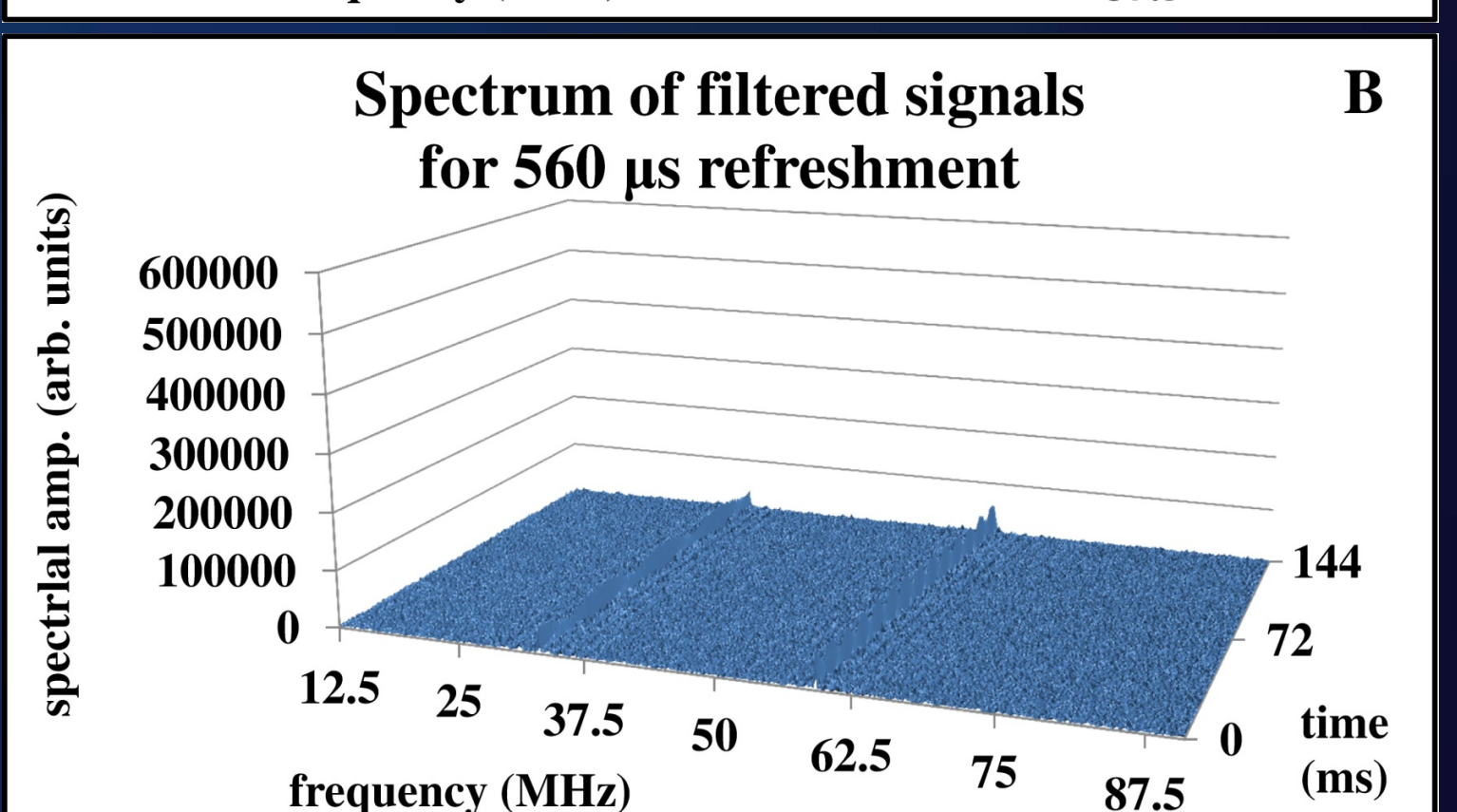
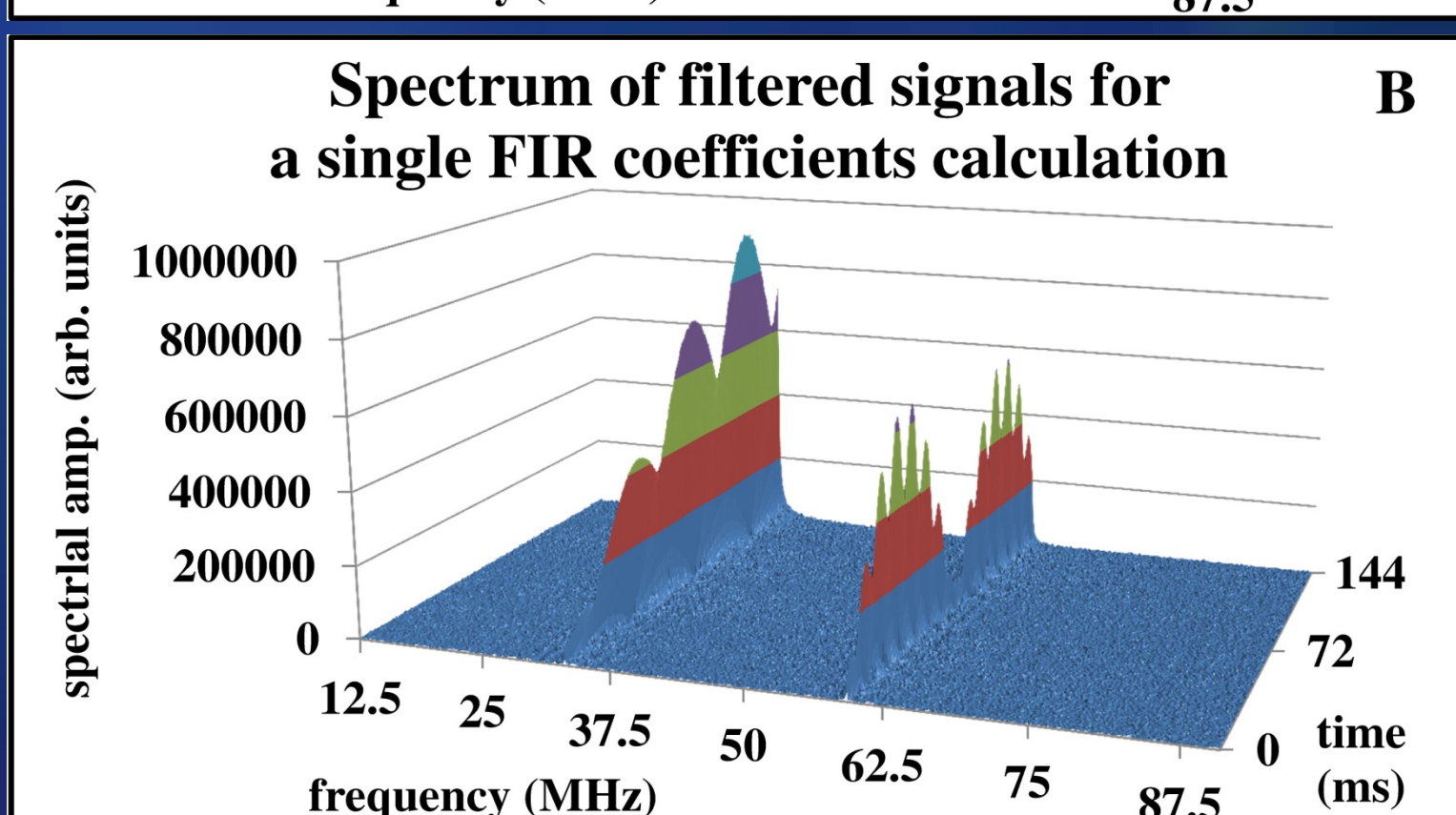
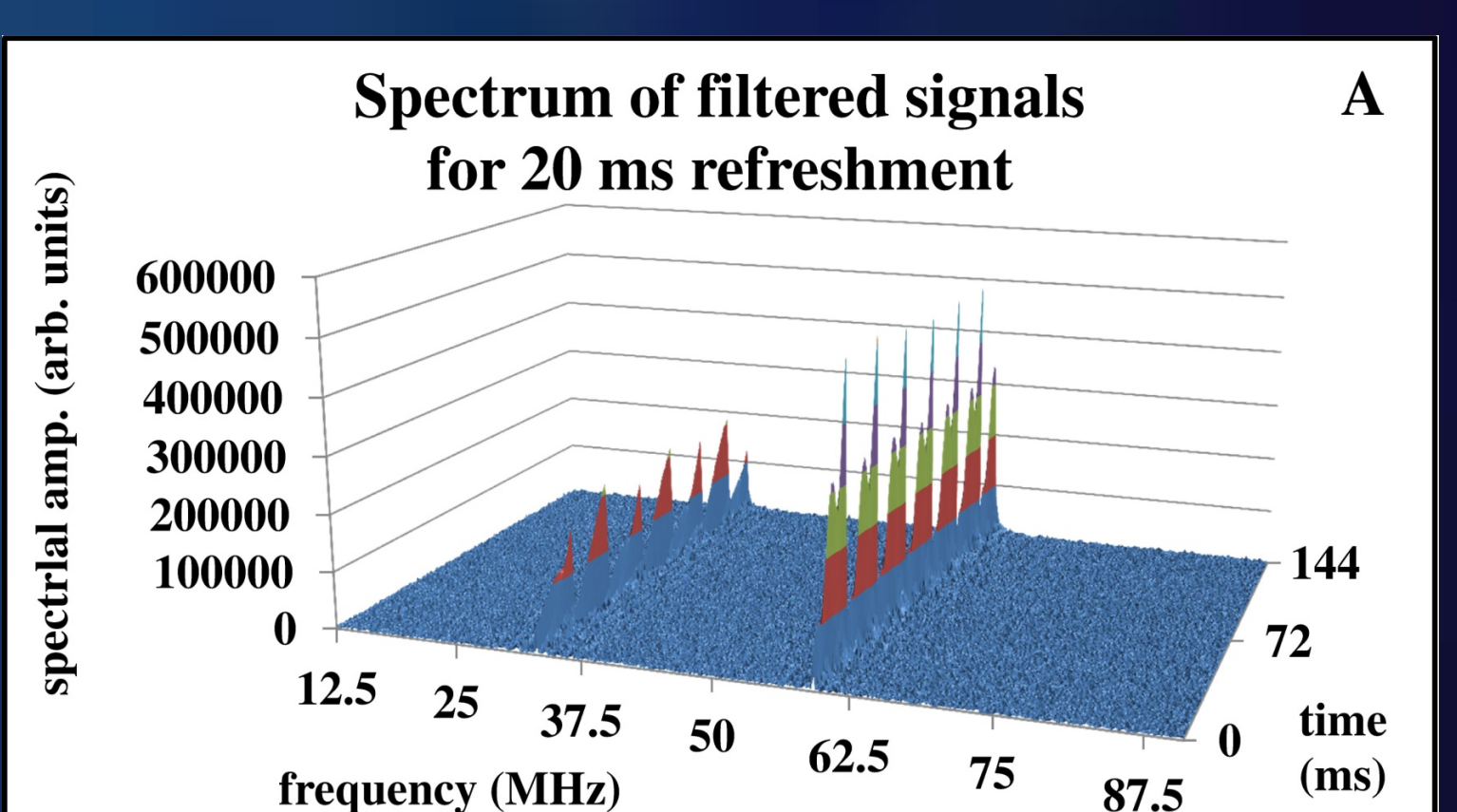
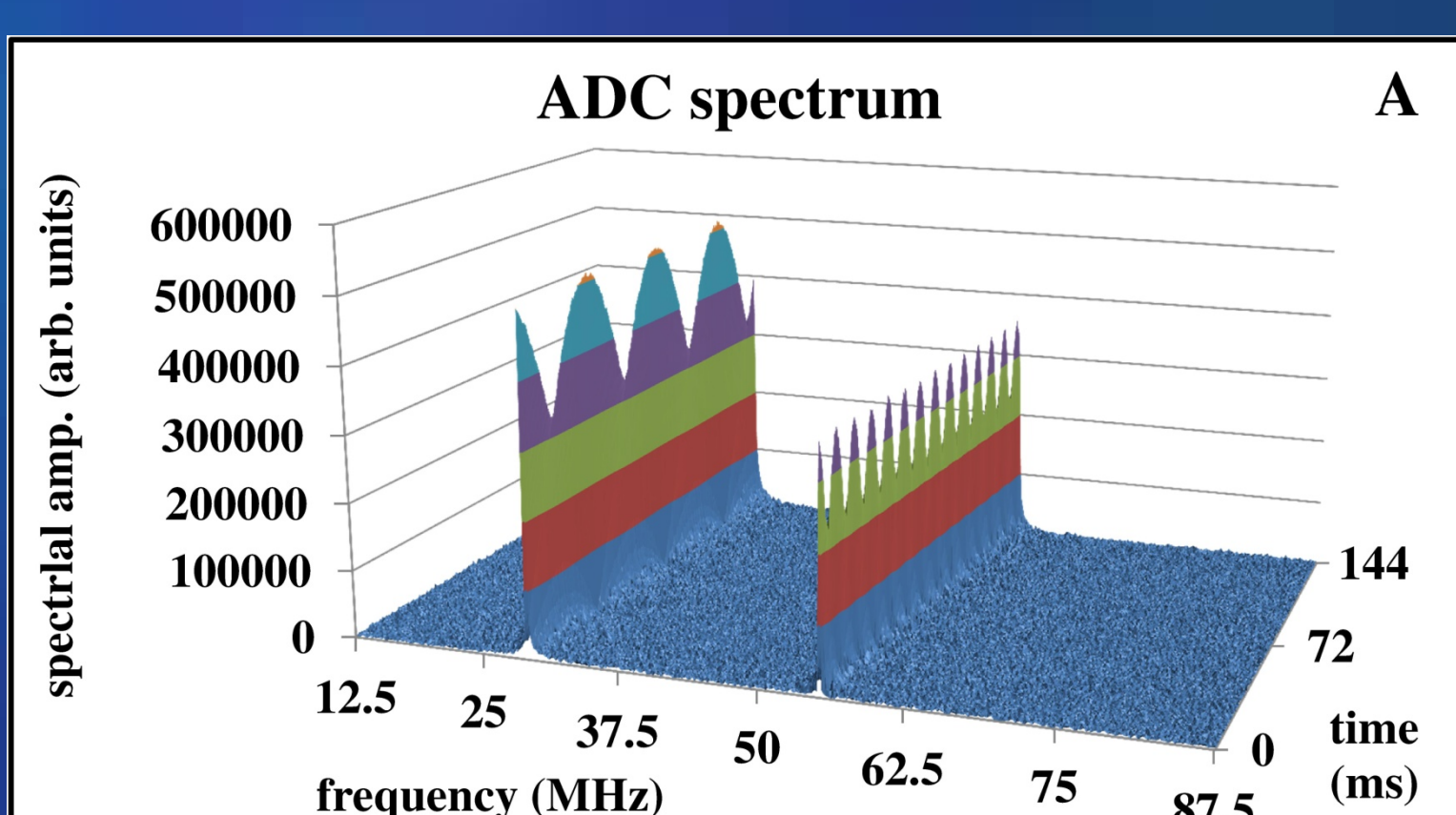


Fig. 11 – Fourier spectra for the original signal (A) and for a single calculation of FIR coefficients in the beginning of trace cleaning (B).

Fig. 12 – Modules of Fourier spectra for the cleaned measured signal 20 ms (A) and 560  $\mu$ s refreshment (B), respectively.

[1] K. Greisen, *End to the cosmic-ray spectrum?*, *Phys. Rev. Lett.* **16** (1966) 748. G. T. Zatsepin, V. A. Kuzmin, *Upper limit of the spectrum of cosmic rays*, *JETP Letters* **4** (1966) 78.  
 [2] J. K. Becker, *High-energy neutrinos in the context of multi-messenger astrophysics*, *Phys. Reports* **458** no. 4-5 (2008) 173.  
 [3] P. Bhattacharjee and G. Sigl, *Origin and propagation of extremely high-energy cosmic rays*, *Phys. Reports* **327** no. 3-4 (2000) 109.  
 [4] V. S. Berezhinsky, A.Yu. Smirnov, *Cosmic neutrinos of ultrahigh energies and detection possibility*, *Astrophys. and Space Sci.* **32** no. 2 (1975) 461.

[5] Z. Szadkowski, *A spectral 1<sup>st</sup> level FPGA trigger for detection of very inclined showers based on a 16-point Discrete Cosine Transform for the Pierre Auger Observatory*, *Nucl. Instrum. Meth. A* **606** (2009) 330.  
 [6] Z. Szadkowski, *Optimization of the Detection of Very Inclined Showers Using a Spectral DCT Trigger in Arrays of Surface Detectors*, *IEEE Trans. on Nucl. Science* **60** (2013) 3647.  
 [7] Z. Szadkowski, K. Pytel, *Artificial Neural Network as a FPGA Trigger for a Detection of Very Inclined "Young" Showers*, *IEEE Trans. on Nucl. Science* **62** Issue 3 (2015) 1002.

## CONCLUSIONS

The hardware Levinson procedure implemented into FPGA fabric significantly shortens the refreshment time in the linear predictor approach used for RFI suppression. With Cyclone® IV (FPGA used at present in the Dutch AERA digitizers) and in Cyclone® V E (considered as FPGA for the future upgrade) the refreshment time is on a level of 560  $\mu$ s (with 100 MHz clock for covariances calculation and the Levinson recursion). The 200 MHz speed has been achieved in the Stratix® III FPGAs (speed grade - 2) and allowed a reduction of refreshment time to 275  $\mu$ s, however, the Stratix® series are too power consuming and too expensive. We plan to use the above algorithm for tests of RFI suppression: a) in Łódź environment using the standard AERA antenna and b) in real radio stations on Argentinean pampas.

This work was supported by the National Science Centre (Poland) under NCN Grant No. 2013/08/M/ST9/00322